

The impact of gamma-ray propagation effects on indirect dark matter searches

**Ignacio Martínez López,^{a,b} Rafael Alves Batista,^{a,c,d,e}
Miguel A. Sánchez-Conde,^{a,c} Antonio Juan
Rubio-Montero^b**

^aDepartamento de Física Teórica, Mod. 15, Universidad Autónoma de Madrid, E-28049 Madrid, Spain.

^bCentro de Investigaciones Energéticas, Medioambientales y Tecnológicas (CIEMAT), Dept. de Tecnología, Av. Complutense 40, Madrid, Spain

^cInstituto de Física Teórica, IFT UAM-CSIC, Calle Nicolás Cabrera 13-15, Campus de Cantoblanco, E-28049 Madrid, Spain.

^dSorbonne Université, Institut d'Astrophysique de Paris, CNRS UMR 7095, 98 bis bd Arago 75014, Paris, France

^eSorbonne Université, Laboratoire de Physique Nucléaire et des Hautes Énergies, 4 place Jussieu, 75005, Paris, France

E-mail: ignacio.martinez@ciemat.es

Abstract. In this work, we investigate dark matter (DM) detection in the context of weakly interacting massive particles (WIMPs). Upon annihilation, WIMPs generate cascades of secondary particles through various channels, many of which culminate in the production of gamma rays. As these gamma rays travel toward Earth, their spectra are reshaped by interactions with the intervening medium. While current models typically account for attenuation via pair production on the extragalactic background light, they often neglect the fate of the resulting electrons and positrons, specifically subsequent inverse Compton scattering of these secondary particles, which can regenerate high-energy gamma rays. Here, we revisit the predicted gamma-ray fluxes from WIMP annihilation by performing a more detailed treatment of propagation effects. We show that for distant sources and annihilation channels such as $\tau^+\tau^-$, the full treatments can significantly alter the observed gamma-ray flux, by up to a factor of three orders of magnitude for heavy WIMPs. This has an impact on current dark matter limits derived without taking into account propagation effects, depending on the considered WIMP mass and annihilation channel. Our study demonstrates the importance of a detailed propagation treatment for indirect dark matter searches, and the need to account for such effects in order to obtain accurate, more reliable dark matter signal predictions and exclusion limits.

Keywords: dark matter simulations, gamma ray theory, gamma ray experiments, galaxy clusters

ArXiv ePrint: [2505.XXXXX](https://arxiv.org/abs/2505.XXXXX)

Contents

1	Introduction	1
2	Dark matter-induced gamma-ray signals	3
2.1	CosmiXs: Gamma-Ray Flux from DM Annihilation	4
3	Propagation Effects on Gamma Rays from DM Annihilation	5
3.1	CRPropa: treatment of propagation effects	7
4	Results	8
4.1	Generic study	8
4.2	The case of Perseus galaxy cluster	9
4.3	Impact on DM limits	9
5	Discussion	12
6	Conclusions and Outlook	14

1 Introduction

Unveiling the nature of dark matter (DM) remains one of the central challenges in modern cosmology and particle physics. While a wide array of astrophysical observations – from galactic rotation curves to gravitational lensing and cosmic microwave background anisotropies – confirm its presence, the particle identity of DM is still unknown [1, 2].

Among the most extensively studied candidates are weakly interacting massive particles (WIMPs), motivated, among other reasons, by the so-called “WIMP miracle”: the observation that particles with masses and interaction cross sections typical of the electroweak scale naturally yield a relic abundance consistent with current measurements [3–6]. Although WIMPs do not arise within the Standard Model (SM), they are predicted in a range of theories beyond the Standard Model (BSM). Supersymmetric (SUSY) models, for instance, introduce a superpartner for each SM particle, and the lightest neutralino has long been a prototypical WIMP candidate [7, 8]. However, recent results from the Large Hadron Collider (LHC) have excluded large portions of the SUSY parameter space, ruling out WIMP candidates in the mass range from a few GeV to several TeV [9].

Other BSM scenarios also predict viable WIMP candidates and are being actively explored through both direct detection experiments and high-energy colliders. Universal extra dimension (UED) models predict the existence of Kaluza-Klein (KK) particles, whose lightest excitation can serve as a stable WIMP candidate [10–12]. Similarly, Little Higgs models with a discrete T-parity symmetry stabilise new particles that can fulfil the role of DM [13–16]. The Minimal Dark Matter framework

extends the SM with additional $SU(2)_L$ multiplets, leading to neutral components that are stable due to accidental symmetries [17]. All of these models are under scrutiny in current and future collider searches, as they predict distinctive signatures beyond those expected from SUSY alone.

Given the lack of conclusive evidence from collider [18, 19] and direct detection experiments [20] so far, indirect detection has become an increasingly important avenue to test the WIMP paradigm. This approach seeks astrophysical signals resulting from DM annihilation or decay in regions of high density [21, 22], such as galactic centres [23–26], dwarf galaxies [27–31], galaxy clusters [32, 33], or dark satellites [34–37], where the interaction rate is expected to be enhanced. Observations are carried out using space-based telescopes like the Fermi Large Area Telescope (Fermi-LAT) [38–40], as well as ground-based Imaging Atmospheric Cherenkov Telescopes (IACTs) [41–48], providing complementary coverage over a broad energy range.

Regarding the astrophysical messengers used for indirect DM detection, gamma rays are particularly useful because, unlike charged cosmic rays, they are not deflected by magnetic fields and thus retain directional information about their sources [31, 49]. Meanwhile, cosmic rays provide complementary constraints on high-energy astrophysical processes [50] and, on the other hand, given that neutrinos can escape from dense regions due to their weakly interacting nature, they offer a unique probe of obscure environments potentially associated with DM [51], despite the difficulty in their detection.

The complementarity of current gamma-ray instruments allows for a broad coverage of the energy range relevant to dark matter (DM) searches. Imaging Atmospheric Cherenkov Telescopes (IACTs), such as MAGIC, provide leading constraints at multi-TeV energies. In particular, the MAGIC collaboration has derived upper limits on the annihilation cross section into monochromatic photons at the level of $\langle\sigma v\rangle \lesssim 5 \times 10^{-28} \text{ cm}^3 \text{ s}^{-1}$ at 1 TeV and $\langle\sigma v\rangle \lesssim 1 \times 10^{-25} \text{ cm}^3 \text{ s}^{-1}$ at 100 TeV [52].

At lower masses, the most robust and constraining limits are currently provided by Fermi-LAT observations of dwarf spheroidal galaxies, which reach the thermal relic cross section, $\langle\sigma v\rangle \sim 3 \times 10^{-26} \text{ cm}^3 \text{ s}^{-1}$ around $m_\chi \sim 100 \text{ GeV}$ for several annihilation channels [30]. For heavy WIMPs, ground-based wide field-of-view observatories such as LHAASO and HAWC further extend sensitivity to DM candidates in the multi-TeV to PeV range [53, 54].

Looking ahead, the forthcoming Cherenkov Telescope Array Observatory (CTAO) is expected to significantly advance these efforts [45]. Designed as a next-generation ground-based observatory with sites in both hemispheres, CTAO will greatly improve upon the capabilities of current instruments by offering enhanced sensitivity, wider energy coverage (from a few tens of GeV up to several hundreds of TeV), improved angular and energy resolution, and faster response times. These advancements will enable more stringent tests of DM models and provide broader opportunities for discovery in the very-high-energy regime.

While ground and space-based instruments provide critical observational constraints on DM through the detection of high-energy gamma rays, interpreting these observations requires a detailed understanding of how such photons propagate through

the Universe. Many DM annihilation channels produce gamma rays that must traverse the intergalactic medium before reaching our detectors. Along the way, these high-energy photons interact with pervasive radiation fields (for a recent comprehensive review see [55]), including the cosmic microwave background (CMB) [56], extragalactic background light (EBL) [57], and cosmic radio background (CRB) [58]. These interactions reshape the energy spectrum originally emitted by the DM source, particularly at the highest energies. Therefore, a robust interpretation of observational data hinges on accurately modelling the effects of these backgrounds on gamma-ray propagation.

The main goal of the present work is to address the impact of gamma-ray propagation effects on indirect DM searches. Indeed, most indirect DM searches consider only gamma-ray attenuation by EBL photons, neglecting secondary gamma-ray production via inverse Compton scattering. In this work, we investigate the impact of including both pair production and inverse Compton scattering with CMB and EBL, and show how this modifies the predictions for DM annihilations signals in the gamma-ray energy range.

We structure our analysis as follows. In Section 2, we describe the methods used to characterise the intrinsic gamma-ray spectrum generated by DM annihilation and outline the computational approach employed using CosmiXs [59]. Section 3 then presents the propagation framework based on CRPropa 3 [60, 61], which incorporates the main physical processes affecting gamma rays in transit. Our results are presented in Section 4, including a general scenario (Subsection 4.1), a specific case involving the Perseus galaxy cluster (Subsection 4.2), and the resulting impact on constraints set on DM particle properties (Subsection 4.3). Finally, we discuss the broader implications of these findings in Section 5.

2 Dark matter-induced gamma-ray signals

In this section, we characterise the flux of gamma rays resulting from DM annihilation, which primarily occurs in DM-dense regions such as galactic haloes and galaxy clusters. Note that we focus solely on WIMPs annihilation and ignore the flux from WIMP decay because we expect the cross section of WIMPs to correspond to the thermal freeze-out [62, 63], while in the case of decay we have no clues of the corresponding interaction rate (although approaches are made to the decay lifetime [64, 65]); thus, annihilation is currently considered a more viable approach to probe the nature of DM.

The differential flux of gamma rays from DM annihilation, observed within a solid angle $\Delta\Omega$, is given by [35, 66]:

$$F = \left(\frac{x\langle\sigma v\rangle}{8\pi} \frac{1}{m_\chi^2} \sum_f \mathcal{B}_f \int_{E_{\text{th}}}^E \frac{dN_\gamma^f}{dE_\gamma} dE_\gamma \right) J_T, \quad (2.1)$$

where $x = 1$ if DM is a Majorana particle and $x = 1/2$ otherwise. Here, $\langle\sigma v\rangle$ denotes the velocity-averaged annihilation cross section for DM particles with mass m_χ , $\frac{dN_\gamma^f}{dE_\gamma}$

is the gamma-ray yield per annihilation to a fermionic final state f , and \mathcal{B}_f is the corresponding branching ratio.

The annihilation process is schematically represented as:

$$\chi\chi \rightarrow \underbrace{[X_1 X_2 \dots X_N]}_{\text{intermediate states}} \rightarrow \overbrace{(Y_{11} \dots Y_{1a_1}) \dots (Y_{N1} \dots Y_{Na_N})}^{\text{stable particles}}, \quad (2.2)$$

where χ represents DM particles, the intermediate states denote annihilation channels, and the resulting stable products are $Y_{N_1} \dots Y_{N_{a_N}}$. We assume that WIMPs predominantly annihilate through a single final state, such that $\mathcal{B}_f = 1$. The limits of integration correspond to the detector's energy threshold (E_{th}), and to an upper limit E_{max} , selected based on the highest DM mass under consideration. According to recent studies [67], viable WIMP candidates could reach masses up to 150 TeV, consistent with the thermal relic abundance framework. This sets the relevant energy scale for the upper limit of the integral in Eq. 2.1, since the energy of the resulting gamma rays depends on the mass of the DM particle.

Although these terms encode the microscopic properties of DM interactions, the total flux also depends on the astrophysical distribution of DM along the line of sight. The second multiplicative term in Eq. 2.1, the so-called astrophysical J -factor, captures this dependence, as it reflects the square of the DM density ($\rho_{\text{DM}}(r)$) integrated over the source volume and normalised by its distance squared, D^2 :

$$J_T = \frac{1}{4\pi D^2} \int_V \rho_{\text{DM}}^2(r) dV. \quad (2.3)$$

The DM density profile must satisfy constraints based on the nature of DM to realistically describe its distribution in halos. Since the 1990s, the Navarro-Frenk-White (NFW) profile [68] has been widely adopted, though improved N-body cosmological simulations have suggested alternative profiles, depending on the precise halo (or sub-halo) characteristics, e.g. [69–73].

2.1 CosmiXs: Gamma-Ray Flux from DM Annihilation

We employ the CosmiXs code [59] to compute the gamma-ray spectra resulting from WIMP annihilation. CosmiXs builds upon prior work [74–77] using quantum field theory (QFT) and Monte Carlo algorithms [78]. It was designed to calculate the energy spectra of secondary particles resulting from DM annihilation or decay, incorporating quantum electrodynamics (QED) and quantum chromodynamics (QCD) effects.

We use the publicly available tables within CosmiXs [59] to obtain the spectra from DM annihilation for WIMP masses ranging from 5 GeV to 100 TeV. This covers the parameter space for cold DM consistent with thermal freeze-out in the early universe. More precisely, the factor on the left-hand side of Eq. 2.2, shown in parentheses, is extracted from the tables provided by CosmiXs. It is based on their simulations and serves as both a spectral and spatial template for gamma-ray observatories such as the previously mentioned Fermi-LAT and IACTs.

Our analysis focuses on the $b\bar{b}$ and $\tau^+\tau^-$ channels, which are commonly studied alongside the W channel. Figure 1 displays the resulting spectra for multiple WIMP masses within these channels. It is important to note that CosmiXs is used exclusively to compute the prompt particle spectra at the source, $\frac{dN_\gamma^f}{dE_\gamma}$. The remaining factors entering Eq. 2.1, including the astrophysical J -factor and the annihilation cross section, are not calculated within CosmiXs. In this work, these quantities are adopted from dedicated studies in the literature and implemented consistently in our analysis.

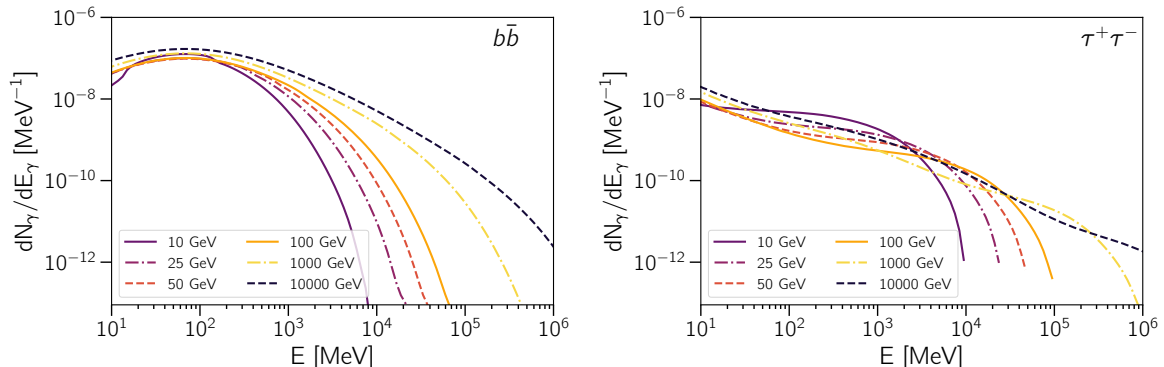


Figure 1. Spectrum of gamma rays produced through the $b\bar{b}$ (left) and $\tau^+\tau^-$ (right panel) annihilation channels (dN_γ/dE_γ), as a function of the energy, for various DM masses.

3 Impact of propagation effects on Gamma-Ray Detection from DM Annihilation

The annihilation of DM particles in a hypothetical dense concentration of WIMPs in the Universe can produce a wide variety of particles. Among them, cosmic rays, neutrinos, and gamma rays stand out. In this work, we focus on gamma-ray detection due to the higher sensitivity of our instruments to them and the fact that gamma rays, being electrically neutral, can be traced back to their sources. However, detecting gamma rays alone is not enough. Interpreting the observed flux requires understanding how these photons evolve on their journey through the Universe. Thus, to fully characterise the energy spectrum of gamma rays from DM annihilation, it is essential to account for propagation effects. As gamma rays travel from the source to Earth, they may interact with pervasive background radiation fields, resulting in a lower flux observed by detectors. Moreover, the adiabatic expansion of the Universe also incurs energy losses.

One of the primary attenuation mechanisms is pair production [79] via interactions with background photons, notably from the CMB, EBL and CRB:

$$\gamma + \gamma_{\text{bg}} \rightarrow e^+ + e^-. \quad (3.1)$$

These produced charged leptons can subsequently undergo inverse Compton scattering [80], transferring energy back to background photons:

$$e^\pm + \gamma_{\text{bg}} \rightarrow e^\pm + \gamma. \quad (3.2)$$

The successive occurrence of these interactions forms an electromagnetic cascade.

Additionally, higher-order interactions such as double pair production [81]:

$$\gamma + \gamma_{\text{bg}} \rightarrow e^+ + e^- + e^+ + e^-. \quad (3.3)$$

and triplet pair production [82]:

$$e^\pm + \gamma_{\text{bg}} \rightarrow e^\pm + e^+ + e^-. \quad (3.4)$$

can occur, but with a negligible effect in the energy range we study in this work [83].

The likelihood of such interactions is strongly energy-dependent and is therefore tied to the DM particle mass. This dependence is quantified through the inverse of the mean free path (λ^{-1}), which represents the probability per unit of distance that a photon interacts with the background fields [84]. Figure 2 shows λ^{-1} as a function of gamma-ray energy for interactions with CMB, EBL, and CRB, along with the reference distance to the Perseus cluster. This specific distance is highlighted because it corresponds to the source from which we later derive constraints on the WIMP mass and annihilation cross section as an example of the impact of gamma-ray propagation effect for DM searches.

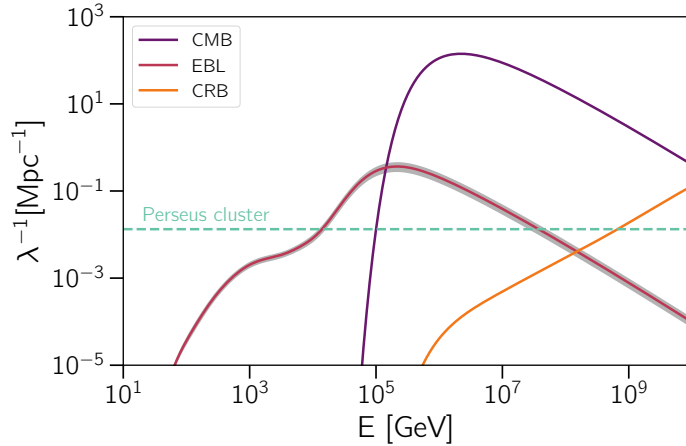


Figure 2. Inverse mean free path (λ^{-1}) of gamma rays as a function of energy. The purple curve represents interactions with the CMB. The red shaded band represents the uncertainty range of the EBL model [85], corresponding to the lower and upper limits derived from observational constraints. The central line indicates the best-fit model, and the contribution from the CRB is also shown in orange. Data from ref [86]. The blue dashed line indicates the inverse distance corresponding to the redshift of the Perseus Cluster ($z \sim 0.017$) [87]. This distance is highlighted due to its role in later sections, where it is used to constrain WIMP properties.

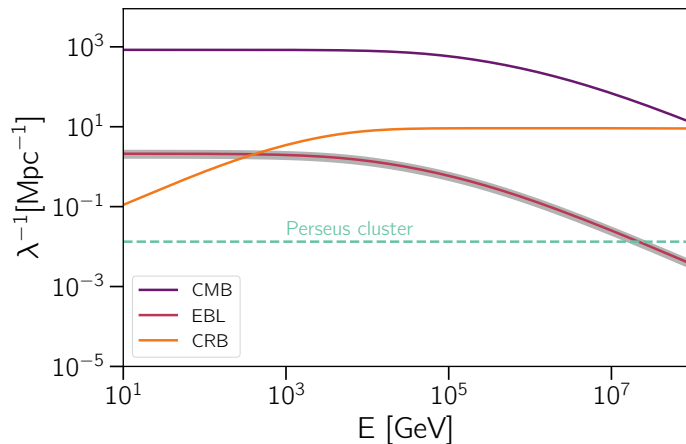


Figure 3. Same as Figure 2, but for inverse Compton scattering between high-energy electrons and background photons from the CMB, EBL, and CRB. The inverse distance to the Perseus cluster is included for reference, as it serves as a benchmark in the analysis of WIMP-induced gamma-ray fluxes presented in later sections.

The attenuation rate for interactions between an arbitrary particle and background photons following Eq.3, as illustrated in Fig. 3, can be written as [84]:

$$\lambda^{-1}(E, z) = \frac{1}{8\beta E^2} \int_0^\infty \int_{s_{\min}}^{s_{\max}} \frac{1}{\epsilon^2} \frac{dn(\epsilon, z)}{d\epsilon} (s - m^2 c^4) \sigma(s - m^2 c^4) ds d\epsilon, \quad (3.5)$$

where ϵ is the energy of the background photon, σ is the cross section of the interaction, and m is the mass of the energetic particle that interacts with these photons. In the case of pair production, $s_{\min} = 4m_e^2 c^4$ and $s_{\max} = 4E\epsilon$. For inverse Compton scattering, $s_{\min} = m_e^2 c^4$ and $s_{\max} = m_e^2 c^4 + 2E\epsilon(1 + \beta)$, with β the speed of the electron in units of c .

Most indirect DM searches consider only attenuation from pair production with EBL photons, neglecting secondary gamma-ray production via inverse Compton scattering. In this work, we investigate the impact of including pair production and inverse Compton scattering with CMB and EBL and show how it modifies our predictions for gamma-ray fluxes from DM annihilation.

3.1 CRPropa: treatment of propagation effects

To model the propagation of gamma rays and their interactions with the cosmological environment, we use the CRPropa code [60, 61]. CRPropa is a Monte Carlo simulation framework designed to track high-energy astrophysical messengers, including cosmic rays, neutrinos, electrons, and gamma rays, as they propagate through intergalactic space.

CRPropa supports both one-dimensional (1D) and three-dimensional (3D) propagation. In this work, we use the 1D mode to treat interactions and energy-loss processes while neglecting magnetic field effects [88]. Redshift energy losses are included, whereas

higher-order interactions, such as double and triplet pair production, although available in CRPropa, are not considered in our simulations. Higher-order interactions such as double and triplet pair production are neglected, as their contribution is subdominant in the TeV energy range considered here. Their cross sections are significantly smaller than those of standard pair production and inverse Compton scattering, becoming relevant only at ultra-high energies (see e.g. [89, 90]).

To study the full propagation history, we use gamma-ray spectra generated by CosmiXs to reweight the propagation simulations of CRPropa. Each simulation tracks a “candidate” particle that evolves through successive steps based on physical modules that simulate interactions, energy losses, and redshift effects. Simulations are terminated when the particle reaches the observer or falls below a minimum energy threshold, set to 1 GeV in our work.

We simulated approximately 10^6 gamma-ray events per configuration, with initial energies extending up to 120 TeV, consistent with the upper range of DM particle mass predictions in supersymmetric models. The propagation distances range from 5 Mpc to 600 Mpc. Step sizes vary dynamically between 0.01 kpc and 100 kpc depending on the local interaction rate. The EBL model used is that of Saldaña-López et al. [85].

This approach allows us to simulate electromagnetic cascades resulting from DM annihilation, and to evaluate the impact of secondary gamma rays produced via inverse Compton scattering, a factor often omitted in conventional analysis, but shown here to play a crucial role in shaping the observed spectra.

4 Results

This section shows the key findings of our analysis, focusing on the gamma-ray spectra obtained after simulating WIMP-induced signals. We build upon earlier sections by applying the combined framework introduced in this work, linking the gamma-ray yields from WIMP annihilation to their subsequent propagation through cosmological distances. Specifically, we used CosmiXs¹ to generate the prompt spectra for various annihilation channels, and CRPropa 3.2.1² to model the effects of interactions during transit. The resulting spectra, shaped by energy losses and deflections, are presented and discussed with an emphasis on potential observational signatures.

Subsection 4.1 focuses on a generic case where the flux is shown in dimensionless units. Subsequently, Subsection 4.2 examines a well-known astrophysical target, the Perseus galaxy cluster. Finally, in Subsection 4.3, we explore how propagation effects can influence constraints on the expected annihilation cross section of WIMPs, using the Perseus gamma-ray spectra as our example case.

4.1 Generic study

To evaluate the role of inverse Compton scattering in the propagation of gamma rays from DM sources, we simulate with CRPropa the gamma-ray flux from two annihilation

¹Git commit [150786c](#)

²Git commit [80bef3b](#)

channels, representative each of them of leptonic and hadronic ‘families’, namely $\tau^+\tau^-$ and $b\bar{b}$, respectively. We analyse four representative distances: 0.5 Mpc (e.g., NGC 6822, the Barnard’s Galaxy) [91], 5 Mpc (e.g., the Sculptor galaxy [92]), 100 Mpc (e.g., the Perseus galaxy cluster [93]), and 600 Mpc (e.g., the Abell 2029 galaxy cluster [94]). As discussed in Subsection 3.1, we expect the observed spectrum to resemble the initial one for nearby sources. In contrast, gamma rays originating from more distant sources undergo multiple interactions with background photons, such as those from the CMB, EBL, or CRB, which progressively reduce their energy. However, in our simulations, we consider only interactions with the CMB and EBL. At very large distances, many high-energy photons fall below the range of energy we are interested in. This effect becomes more pronounced for higher DM masses, as shown in Figures 2 and 3.

These propagation effects are particularly relevant for DM masses in the TeV range and become negligible in the GeV range unless travelling very long distances. For this reason, we simulate masses $m_\chi = 1, 10, 100$ TeV. The results are shown in Figures 4 and 5. Figure 4 displays the intrinsic spectrum of annihilation and the resulting dimensionless flux after propagation over various distances for all interactions mentioned in Subsection 3.1, including inverse Compton scattering and pair production. Figure 5 shows the ratio between fluxes calculated with inverse Compton scattering and in the absence of inverse Compton scattering for the same scenarios.

4.2 The case of Perseus galaxy cluster

After analysing generic distances, we now focus on the well-known Perseus galaxy cluster, located at redshift $z \sim 0.017$ [87].

Figure 6 shows the flux ratio with (ICS) and without (nICS) inverse Compton scattering, labelled ($F_{\text{ICS}}/F_{\text{nICS}}$), for Perseus cluster and various DM masses and annihilation channels. While in the previous subsection we appreciate the relation between the flux ratio and the distance that gamma rays travel, in this case the results show how the WIMP mass affects this ratio, given that the distance is fixed. This figure seems to show a behaviour similar to the 100 Mpc cases in Fig. 5, since this is approximately the distance to the cluster.

4.3 Impact on DM limits

To quantify the impact of inverse Compton scattering on DM exclusion limits, we integrate the normalised gamma-ray flux shown in Figure 6 over a range of WIMP masses m_χ in the Perseus cluster, comparing the results obtained with and without including the contribution from inverse Compton scattering. This procedure yields flux ratios that directly translate into modifications of the exclusion limits on $\langle\sigma v\rangle$, as illustrated in Figure 7. The results displayed in this figure were derived using as a reference an energy range (0.05-100 TeV) within the projected sensitivity of the CTAO from Ref. [95], and applying the factor corresponding to the difference between including and neglecting inverse Compton scattering. The obtained results suggest that a more detailed treatment of propagation does not lead to substantial changes in the main DM observable, namely the velocity-averaged annihilation cross section.

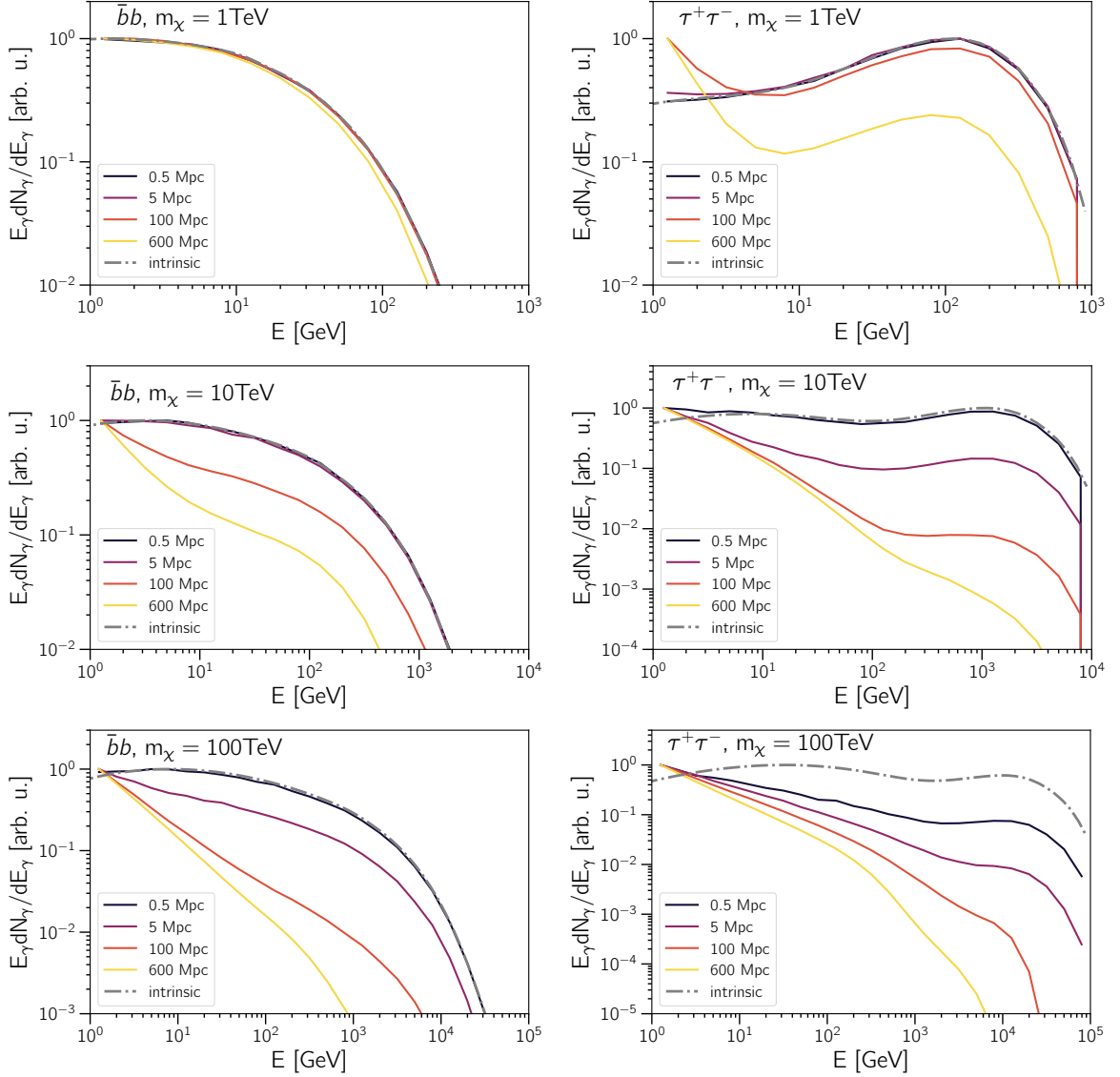


Figure 4. Simulated dimensionless gamma-ray flux, expressed as $E \frac{dN}{dE}$, as a function of energy (in GeV) for the $\bar{b}b$ annihilation channel (left column) and the $\tau^+\tau^-$ channel (right column). The panels correspond to DM masses of 1 TeV (upper row), 10 TeV (middle row), and 100 TeV (lower row). Dashed gray lines denote the annihilation spectra at the source position, while black, purple, red and yellow solid lines correspond to different source distances, 0.5, 5, 100, and 600 Mpc, respectively. All relevant interactions during propagation are taken into account—including, and more importantly, inverse Compton scattering—which progressively alters the spectral shape as the distance increases.

While this is indeed the case, it strongly depends on the limits of integration over energy in Eq. 2.1. We thus examine the behaviour within specific energy intervals.

To further explore this energy dependence, we repeat the comparison for different energy intervals. The resulting flux ratios and their influence on the limits are shown in Figure 8.

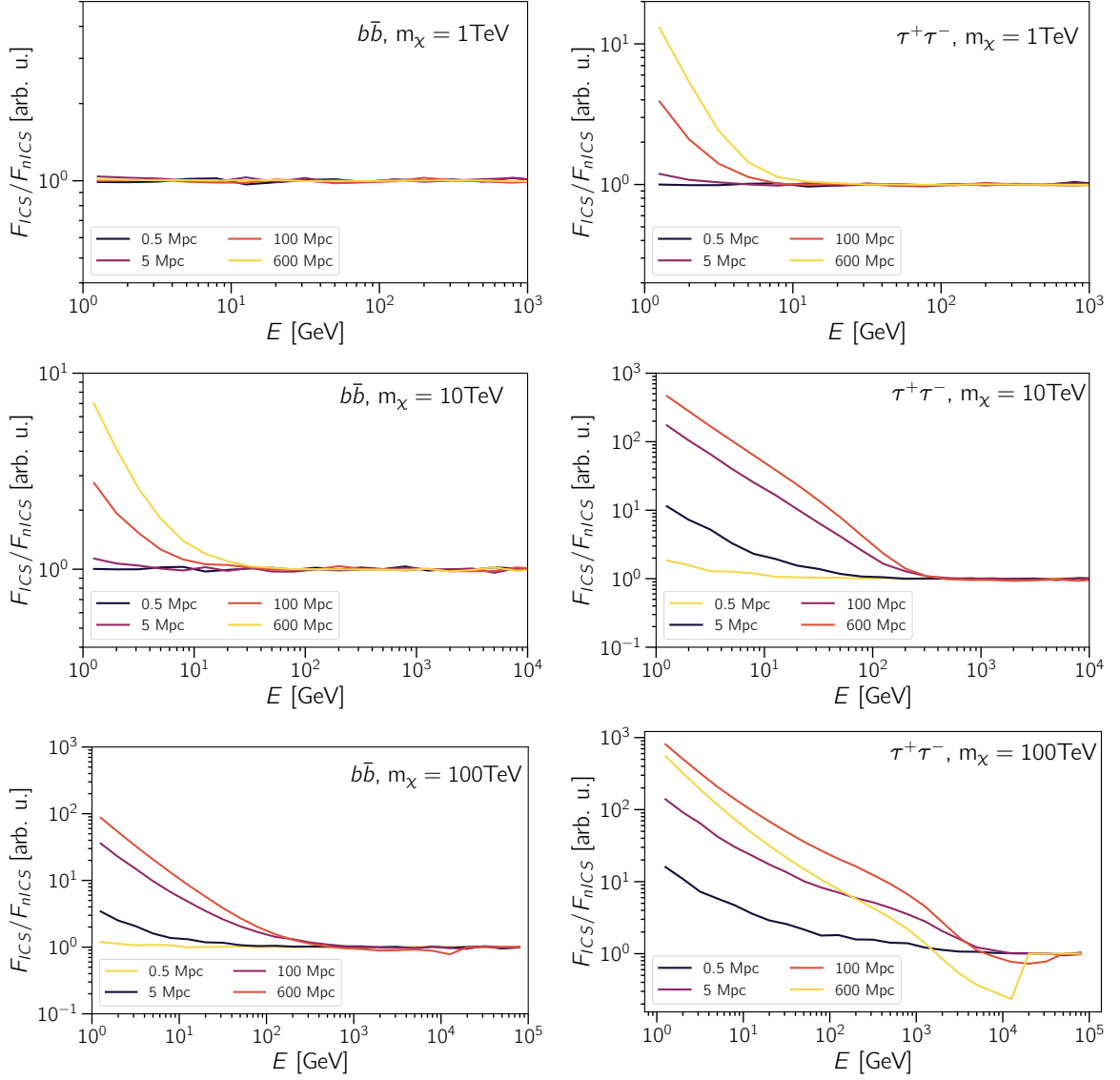


Figure 5. Ratio between the expected fluxes at Earth considering the effects of inverse Compton scattering (ICS) and ignoring it (nICS) (F_{ICS}/F_{nICS}) as a function of energy (in GeV) for $b\bar{b}$ (left) and $\tau^+\tau^-$ (right panels) channels, for different DM masses: 1 TeV (upper panels), 10 TeV (middle), and 100 TeV (lower panels). The black, purple, red and yellow lines correspond to different source distances, 0.5, 5, 100, and 600 Mpc, respectively.

This figure is instructive, as it illustrates how the parameter space evolves with the choice of an observational energy window. In particular, constraints derived from observatories sensitive to ~ 1 –100 GeV energies (e.g., Fermi-LAT) show strong sensitivity to high DM masses for this specific cluster. By contrast, in the $\gtrsim 1$ TeV range, typical of gamma rays detected by IACTs, the impact of propagation effects on the DM limits remains minimal, largely independent of the WIMP mass.

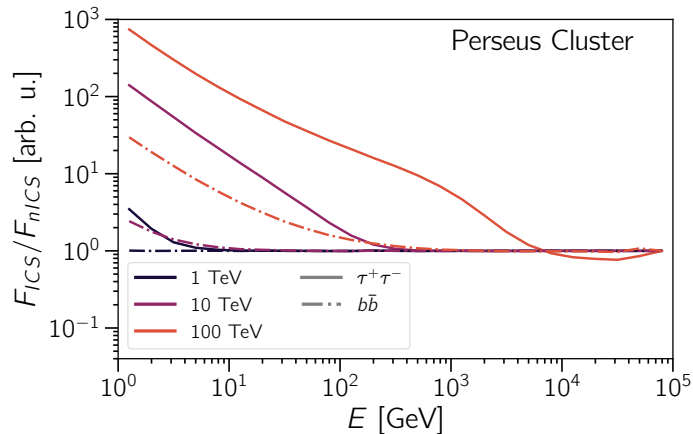


Figure 6. Flux ratio ($F_{\text{ICS}}/F_{\text{nICS}}$) for the Perseus Cluster, as a function of the energy, for the $b\bar{b}$ and $\tau^+\tau^-$ channels. Black, purple and red lines correspond to DM masses of 1, 10, and 100 TeV, respectively.

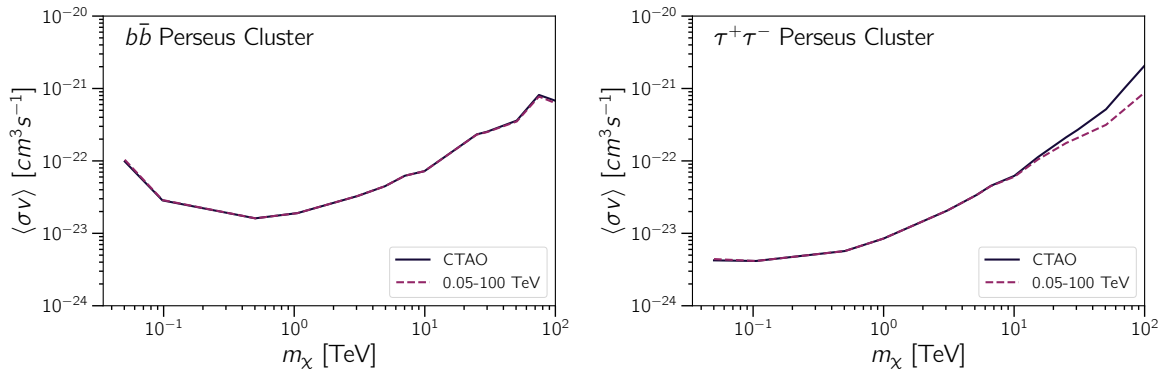


Figure 7. Comparison of the exclusion limits on $\langle\sigma v\rangle$ from this work (red dashed line) and those from Ref. [95] (solid black line).

5 Discussion

The results presented in Section 4 highlight the crucial role of inverse Compton scattering in shaping the gamma-ray spectra originating from WIMP annihilation and observed from Earth. Across the range of WIMP masses and propagation distances studied, we observe that including this process consistently leads to a redistribution of photon energies, resulting in enhanced fluxes at lower energies and a corresponding depletion in the high-energy domain.

More specifically, for higher WIMP masses (e.g., $m_\chi \simeq 100$ TeV) and propagation distances exceeding 100 Mpc, the impact becomes substantial, with flux ratios between simulations with and without inverse Compton scattering reaching values as high as 10^3 in the lower-energy regime. This effect diminishes progressively for lower masses and shorter distances, where the ratio tends toward unity and the spectra remain close to the annihilation spectrum without inverse Compton scattering.

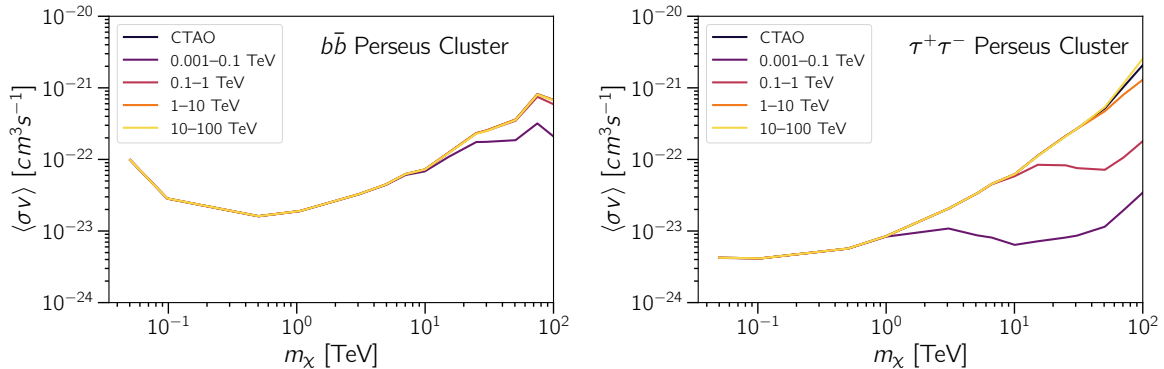


Figure 8. Comparison of the exclusion limits on $\langle\sigma v\rangle$ from Ref. [95] (solid black line) of the gamma-ray energy spectrum and those calculated in this work corresponding to the integration ranges of 0.001 – 0.1 TeV (solid purple line), 0.1 – 1 TeV (solid red line), 1 – 10 TeV (solid orange line), 10 – 100 TeV (solid yellow line).

Some channels are more prone to the regeneration of photons via inverse Compton scattering. While hadronic channels such as $b\bar{b}$ exhibit more moderate deviations, typically up to one order of magnitude, leptonic channels like $\tau^+\tau^-$ display significantly larger differences, particularly for gamma rays arriving at Earth with energies below 1 TeV. These findings are consistent with the higher production rates of high-energy electrons and positrons produced in leptonic annihilation, which are responsible for the signal through the upscattering of background photons from the CMB and EBL.

In the specific case of the Perseus galaxy cluster, the results are similar to the generic scenarios at a similar distance. The flux ratios and modified exclusion limits suggest that these propagation effects are not merely theoretical subtleties, but can have measurable observational consequences. Notably, the shifts in the velocity-averaged DM cross-section constraints for the $\tau^+\tau^-$ channel approach factors of ~ 0.4 for the highest masses considered, confirming that accurate modelling of gamma-ray propagation is essential when interpreting indirect DM detection limits.

Similarly, the interpretation of gamma-ray constraints for superheavy DM candidates with masses above ~ 100 TeV must necessarily account for electromagnetic cascades initiated by their annihilation or decay products. On Galactic scales, interactions of the resulting high-energy photons and electrons with the interstellar radiation field (ISRF), as well as with the CMB and EBL are also important. These interactions reprocess the primary emission through inverse Compton scattering and pair production, softening the spectrum and modifying its observable shape and intensity [96]. Consequently, existing gamma-ray bounds on such superheavy WIMPs may require revision as well. This is left for future work.

Overall, our study highlights the potentially important role of inverse Compton scattering of secondary electrons by background photons – a phenomenon often neglected – which can lead to systematic biases in both the predicted spectra and the derived constraints on DM properties, especially in the high-mass regime and for certain annihilation channels.

Given the energies at which these discrepancies become important, gamma-ray observations in the 1–100 GeV energy range play a crucial role. At present, Fermi-LAT remains the only instrument covering this energy window. For more distant sources and higher DM masses, the effects discussed here may already be detectable with current IACTs.

6 Conclusions and Outlook

In this work, we have developed a framework combining CosmiXs and CRPropa to consistently model both the intrinsic gamma-ray spectra from WIMP annihilation and their modification due to propagation effects. The main novelty is the inclusion of secondary photons produced via inverse Compton scattering generated by pair-produced electrons. Our results demonstrate that accounting for this process significantly alters the predicted fluxes at Earth, with differences spanning up to three orders of magnitude depending on the considered energy range, WIMP mass, and annihilation channel.

For observational facilities such as Fermi-LAT and the upcoming CTAO, which probe precisely the energy ranges most affected by these interactions, our findings imply that inverse Compton scattering must be incorporated into any robust interpretation of gamma-ray data in the context of DM searches. In particular, the shifts in DM exclusion limits and cross-section estimates demonstrate that propagation effects can partially relax constraints previously considered stringent, potentially reopening portions of the WIMP parameter space.

Future work could extend this approach by including additional annihilation channels and by exploring the role of magnetic fields in shaping the secondary emission. Moreover, applying this framework to specific astrophysical targets beyond the one studied in this work could further test the universality of these findings across different environments.

In conclusion, our study highlights the importance of properly accounting for propagation effects in indirect DM searches. By showing how inverse Compton scattering can reshape the predicted DM-induced gamma-ray spectra and modify derived DM constraints, this work underscores that detailed modelling is not just a refinement but a necessity for accurate interpretation of future observations. Indeed, incorporating such effects will be key to obtaining more precise and reliable limits on WIMP properties using gamma-ray data collected by current instruments like Fermi-LAT and upcoming ones like CTAO.

Acknowledgements

This work has been partially co-funded by the Spanish Ministry of Science, Innovation, and Universities through the MINERIA project (Grant ID: PID2024-157169OB-I00). IML gratefully acknowledges CIEMAT for supporting his predoctoral contract. RAB is supported by the Agence Nationale de la Recherche (ANR), project ANR-23-CPJ1-0103-01. The early stages of this work were funded by the “la Caixa” Foundation (ID 100010434) and the European Union’s Horizon 2020 research and innovation

program under the Marie Skłodowska-Curie grant agreement No 847648 (fellowship LCF/BQ/PI21/11830030). The work of MASC was supported by the grants PID2024-155874NB-C21 and CEX2020-001007-S, both funded by MCIN/AEI/10.13039/501100011033 and by “ERDF A way of making Europe”. MASC also acknowledges the MultiDark Network, ref. RED2022-134411-T.

References

- [1] G. Bertone, D. Hooper and J. Silk, *Particle dark matter: evidence, candidates and constraints*, *Phys. Rept.* **405** (2005) 279 [[hep-ph/0404175](#)].
- [2] G. Bertone and D. Hooper, *History of dark matter*, *Rev. Mod. Phys.* **90** (2018) 045002 [[1605.04909](#)].
- [3] P. Gondolo and G. Gelmini, *Cosmic abundances of stable particles: Improved analysis*, *Nucl. Phys. B* **360** (1991) 145.
- [4] K. Griest and D. Seckel, *Three exceptions in the calculation of relic abundances*, *Phys. Rev. D* **43** (1991) 3191.
- [5] M. Srednicki, R. Watkins and K.A. Olive, *Calculations of relic densities in the early universe*, *Nucl. Phys. B* **310** (1988) 693.
- [6] G. Steigman and M.S. Turner, *Cosmological constraints on the properties of weakly interacting massive particles*, *Nucl. Phys. B* **253** (1985) 375.
- [7] H.E. Haber and G.L. Kane, *The search for supersymmetry: Probing physics beyond the standard model*, *Phys. Rept.* **117** (1985) 75.
- [8] L. Roszkowski, E.M. Sessolo and S. Trojanowski, *WIMP dark matter candidates and searches—current status and future prospects*, *Rept. Prog. Phys.* **81** (2018) 066201 [[1707.06277](#)].
- [9] M. Deshpande, J. Hamann, D. Sengupta, M. White, A.G. Williams and Y.Y.Y. Wong, *Revisiting cosmological constraints on supersymmetric SuperWIMPs*, *Eur. Phys. J. C* **84** (2024) 667 [[2309.05709](#)].
- [10] H.-C. Cheng, J.L. Feng and K.T. Matchev, *Kaluza-Klein dark matter*, *Phys. Rev. Lett.* **89** (2002) 211301 [[hep-ph/0207125](#)].
- [11] G. Servant and T.M.P. Tait, *Is the lightest Kaluza-Klein particle a viable dark matter candidate?*, *Nucl. Phys. B* **650** (2003) 391 [[hep-ph/0206071](#)].
- [12] F.J. de Anda, O. Medina, J.W.F. Valle and C.A. Vaquera-Araujo, *Revamping Kaluza-Klein dark matter in an orbifold theory of flavor*, *Phys. Rev. D* **108** (2023) 035046 [[2212.09174](#)].
- [13] Q.-P. Qiao and B. Xu, *Dark matter pair production at the ILC in the Littlest Higgs model with T-parity*, *Chin. Phys. C* **37** (2013) 033103 [[1105.3555](#)].
- [14] N. Arkani-Hamed, A.G. Cohen, E. Katz and A.E. Nelson, *The Littlest Higgs*, *JHEP* **07** (2002) 034 [[hep-ph/0206021](#)].
- [15] T. Han, H.E. Logan, B. McElrath and L.-T. Wang, *Phenomenology of the little Higgs model*, *Phys. Rev. D* **67** (2003) 095004 [[hep-ph/0301040](#)].

- [16] M. Schmaltz and D. Tucker-Smith, *Little Higgs Theories*, *Ann. Rev. of Nucl. Part. Sci.* **55** (2005) 229 [[hep-ph/0502182](#)].
- [17] M. Cirelli, N. Fornengo and A. Strumia, *Minimal dark matter*, *Nucl. Phys. B* **753** (2006) 178 [[hep-ph/0512090](#)].
- [18] A. Boveia and C. Doglioni, *Dark Matter Searches at Colliders*, *Ann. Rev. of Nucl. Part. Sci.* **68** (2018) 429 [[1810.12238](#)].
- [19] L. Lee, C. Ohm, A. Soffer and T.-T. Yu, *Collider searches for long-lived particles beyond the Standard Model*, *Prog. Part. Nucl. Phys.* **106** (2019) 210 [[1810.12602](#)].
- [20] M. Misiaszek and N. Rossi, *Direct Detection of Dark Matter: A Critical Review*, *Symmetry* **16** (2024) 201 [[2310.20472](#)].
- [21] J.M. Gaskins, *A review of indirect searches for particle dark matter*, *Contemp. Phys.* **57** (2016) 496 [[1604.00014](#)].
- [22] R.K. Leane, *Indirect Detection of Dark Matter in the Galaxy*, in *3rd World Summit on Exploring the Dark Side of the Universe*, (Guadeloupe Islands), pp. 203–228, University of Kansas Libraries, 2020 [[2006.00513](#)].
- [23] FERMI-LAT collaboration, *Fermi-LAT Observations of High-Energy γ -Ray Emission Toward the Galactic Center*, *Astrophys. J.* **819** (2016) 44 [[1511.02938](#)].
- [24] FERMI-LAT collaboration, *The Fermi Galactic Center GeV Excess and Implications for Dark Matter*, *Astrophys. J.* **840** (2017) 43 [[1704.03910](#)].
- [25] M. Di Mauro, *Characteristics of the Galactic Center excess measured with 11 years of Fermi-LAT data*, *Phys. Rev. D* **103** (2021) 063029 [[2101.04694](#)].
- [26] J. Zuriaga-Puig, V. Gammaldi, D. Gaggero, T. Lacroix and M.Á. Sánchez-Conde, *Multi-TeV dark matter density in the inner Milky Way halo: spectral and dynamical constraints*, *JCAP* **11** (2023) 063 [[2307.06823](#)].
- [27] FERMI-LAT collaboration, *Searching for Dark Matter Annihilation from Milky Way Dwarf Spheroidal Galaxies with Six Years of Fermi Large Area Telescope Data*, *Phys. Rev. Lett.* **115** (2015) 231301.
- [28] HESS, HAWC, VERITAS, MAGIC, H.E.S.S., FERMI-LAT collaboration, *Combined dark matter searches towards dwarf spheroidal galaxies with Fermi-LAT, HAWC, H.E.S.S., MAGIC, and VERITAS*, *PoS ICRC2021* (2021) 528 [[2108.13646](#)].
- [29] FERMI-LAT collaboration, *Dark Matter search in dwarf irregular galaxies with the Fermi Large Area Telescope*, *PoS ICRC2021* (2021) 509 [[2109.11291](#)].
- [30] A. McDaniel, M. Ajello, C.M. Karwin, M. Di Mauro, A. Drlica-Wagner and M.A. Sánchez-Conde, *Legacy analysis of dark matter annihilation from the Milky Way dwarf spheroidal galaxies with 14 years of Fermi-LAT data*, *Phys. Rev. D* **109** (2024) 063024 [[2311.04982](#)].
- [31] C. Fernández-Suarez and M.A. Sánchez-Conde, *A Search for Dark Matter Annihilation in Stellar Streams with the Fermi-LAT*, *JCAP* **2025** (2025) 003 [[2502.15656](#)].
- [32] FERMI-LAT collaboration, *Search for extended gamma-ray emission from the Virgo galaxy cluster with Fermi-LAT*, *Astrophys. J.* **812** (2015) 159 [[1510.00004](#)].

- [33] M. Di Mauro, J. Pérez-Romero, M.A. Sánchez-Conde and N. Fornengo, *Constraining the dark matter contribution of γ rays in clusters of galaxies using Fermi-LAT data*, *Phys. Rev. D* **107** (2023) 083030 [[2303.16930](#)].
- [34] FERMI-LAT collaboration, *Search for Dark Matter Satellites using the Fermi-LAT*, *Astrophys. J.* **747** (2012) 121 [[1201.2691](#)].
- [35] J. Coronado-Blazquez, M.A. Sanchez-Conde, A. Dominguez, A. Aguirre-Santaella, M. Di Mauro, N. Mirabal et al., *Unidentified Gamma-ray Sources as Targets for Indirect Dark Matter Detection with the Fermi-Large Area Telescope*, *JCAP* **07** (2019) 020 [[1906.11896](#)].
- [36] FERMI-LAT collaboration, *Spectral and spatial analysis of the dark matter subhalo candidates among fermi large area telescope unidentified sources*, *JCAP* **2019** (2019) 045 [[2204.00267](#)].
- [37] FERMI-LAT collaboration, *Spatial extension of dark subhalos as seen by fermi-lat and the implications for wimp constraints*, *Phys. Rev. D* **105** (2022) 083006 [[2204.00267](#)].
- [38] FERMI-LAT collaboration, *The Large Area Telescope on the Fermi Gamma-ray Space Telescope Mission*, *Astrophys. J.* **697** (2009) 1071 [[0902.1089](#)].
- [39] J. Conrad, J. Cohen-Tanugi and L.E. Strigari, *WIMP searches with gamma rays in the Fermi era: challenges, methods and results*, *J. Exp. Theor. Phys.* **121** (2015) 1104 [[1503.06348](#)].
- [40] FERMI-LAT collaboration, *Sensitivity Projections for Dark Matter Searches with the Fermi Large Area Telescope*, *Phys. Rept.* **636** (2016) 1 [[1605.02016](#)].
- [41] T.C. Weekes et al., *VERITAS: The Very energetic radiation imaging telescope array system*, *Astropart. Phys.* **17** (2002) 221 [[astro-ph/0108478](#)].
- [42] E. Lorenz, *Status of the 17 m magic telescope*, *New Astron. Rev.* **48** (2004) 339.
- [43] J. Hinton, *The status of the hess project*, *New Astron. Rev.* **48** (2004) 331.
- [44] HAWC collaboration, *The 2HWC HAWC Observatory Gamma Ray Catalog*, *Astrophys. J.* **843** (2017) 40 [[1702.02992](#)].
- [45] CTA collaboration, *Science with the Cherenkov Telescope Array*, WSP (11, 2018), [10.1142/10986](#), [[1709.07997](#)].
- [46] LHAASO collaboration, *Lhaaso instruments and detector technology*, *Chin. Phys. C* **46** (2022) 030001.
- [47] R. Mukherjee and R. Zanin, *Advances in Very High Energy Astrophysics: The Science Program of the Third Generation IACTs for Exploring Cosmic Gamma Rays*, World Scientific, Singapore (2024), [10.1142/11141](#).
- [48] SWGO collaboration, *Science Prospects for the Southern Wide-field Gamma-ray Observatory: SWGO*, [2506.01786](#).
- [49] CTA collaboration, *Search for dark matter with IACTs and the Cherenkov Telescope Array*, *J. Phys. Conf. Ser.* **2429** (2023) 012019 [[2302.11318](#)].
- [50] P. Salati, *What charged cosmic rays tell us on dark matter*, *SciPost Phys. Proc.* **12** (2023) 067 [[2210.07166](#)].

- [51] SUPER-KAMIOKANDE collaboration, *Indirect search for dark matter from the Galactic Center and halo with the Super-Kamiokande detector*, *Phys. Rev. D* **102** (2020) 072002 [[2005.05109](#)].
- [52] MAGIC collaboration, *Search for Gamma-Ray Spectral Lines from Dark Matter Annihilation up to 100 TeV toward the Galactic Center with MAGIC*, *Phys. Rev. Lett.* **130** (2023) 061002 [[2212.10527](#)].
- [53] HAWC collaboration, *Dark Matter Limits From Dwarf Spheroidal Galaxies with The HAWC Gamma-Ray Observatory*, *Astrophys. J.* **853** (2018) 154 [[1706.01277](#)].
- [54] LHAASO collaboration, *Constraints on Heavy Decaying Dark Matter from 570 Days of LHAASO Observations*, *Phys. Rev. Lett.* **129** (2022) 261103 [[2210.15989](#)].
- [55] S.P. Driver, *Measuring energy production in the Universe over all wavelengths and all time*, in *IAU Symposium 355: The Realm of the Low Surface Brightness Universe*, 2, 2021 [[2102.12089](#)].
- [56] J.C. Mather, E.S. Cheng, D.A. Cottingham, R.E. Eplee, Jr., D.J. Fixsen, T. Hewagama et al., *Measurement of the Cosmic Microwave Background Spectrum by the COBE FIRAS Instrument*, *Astrophys. J.* **420** (1994) 439.
- [57] A. Franceschini and G. Rodighiero, *The extragalactic background light revisited and the cosmic photon-photon opacity*, *Astron. Astrophys.* **603** (2017) A34 [[1705.10256](#)].
- [58] D.J. Fixsen et al., *ARCADE 2 Measurement of the Extra-Galactic Sky Temperature at 3-90 GHz*, *Astrophys. J.* **734** (2011) 5 [[0901.0555](#)].
- [59] C. Arina, M. Di Mauro, N. Fornengo, J. Heisig, A. Jueid and R.R. de Austri, *CosmiXs: cosmic messenger spectra for indirect dark matter searches*, *JCAP* **03** (2024) 035 [[2312.01153](#)].
- [60] R. Alves Batista, A. Dundovic, M. Erdmann, K.-H. Kampert, D. Kuempel, G. Müller et al., *CRPropa 3—a public astrophysical simulation framework for propagating extraterrestrial ultra-high energy particles*, *JCAP* **05** (2016) 038 [[1603.07142](#)].
- [61] R. Alves Batista, J. Becker Tjus, J. Dörner, A. Dundovic, B. Eichmann, A. Frie et al., *CRPropa 3.2 - an advanced framework for high-energy particle propagation in extragalactic and galactic spaces*, *JCAP* **2022** (2022) 035 [[2208.00107](#)].
- [62] S. Dodelson and F. Schmidt, *Modern Cosmology*, Academic Press (2020).
- [63] G. Steigman, B. Dasgupta and J.F. Beacom, *Precise Relic WIMP Abundance and its Impact on Searches for Dark Matter Annihilation*, *Phys. Rev. D* **86** (2012) 023506 [[1204.3622](#)].
- [64] C. Arina, T. Hambye, A. Ibarra and C. Weniger, *Intense gamma-ray lines from hidden vector dark matter decay*, *JCAP* **2010** (2010) 024 [[0912.4496](#)].
- [65] V.A. Acciari, S. Ansoldi, L.A. Antonelli, A. Arbet Engels, C. Arcaro, D. Baack et al., *Constraining dark matter lifetime with a deep gamma-ray survey of the Perseus galaxy cluster with MAGIC*, *Phys. Dark Univ.* **22** (2018) 38 [[1806.11063](#)].
- [66] L. Bergstrom, P. Ullio and J.H. Buckley, *Observability of gamma-rays from dark matter neutralino annihilations in the Milky Way halo*, *Astropart. Phys.* **9** (1998) 137 [[astro-ph/9712318](#)].

- [67] R. Frumkin, E. Kuflik, I. Lavie and T. Silverwater, *Roadmap to Thermal Dark Matter beyond the Weakly Interacting Dark Matter Unitarity Bound*, *Phys. Rev. Lett.* **130** (2023) 171001 [2207.01635].
- [68] J.F. Navarro, C.S. Frenk and S.D.M. White, *The Structure of Cold Dark Matter Halos*, *Astrophys. J.* **462** (1996) 563 [astro-ph/9508025].
- [69] J. Einasto, *On the Construction of a Composite Model for the Galaxy and on the Determination of the System of Galactic Parameters*, *Trudy Astrofizicheskogo Instituta Alma-Ata* **5** (1965) 87.
- [70] L. Hernquist, *An Analytical Model for Spherical Galaxies and Bulges*, *Astrophys. J.* **356** (1990) 359.
- [71] E. Retana-Montenegro, E. Van Hese, G. Gentile, M. Baes and F. Frutos-Alfaro, *Analytical properties of Einasto dark matter haloes*, *Astron. Astrophys.* **540** (2012) A70 [1202.5242].
- [72] A. Di Cintio, C.B. Brook, A.V. Macciò, G.S. Stinson, A. Knebe, A.A. Dutton et al., *The dependence of dark matter profiles on the stellar-to-halo mass ratio: a prediction for cusps versus cores*, *Mon. Not. Roy. Astron. Soc.* **437** (2014) 415 [1306.0898].
- [73] R. Errani and J.F. Navarro, *The asymptotic tidal remnants of cold dark matter subhaloes*, *Mon. Not. Roy. Astron. Soc.* **505** (2021) 18 [2011.07077].
- [74] M. Cirelli, G. Corcella, A. Hektor, G. Hütsi, M. Kadastik, P. Panci et al., *PPPC 4 DM ID: a poor particle physicist cookbook for dark matter indirect detection*, *JCAP* **2011** (2011) 051 [1012.4515].
- [75] P. Ciafaloni, D. Comelli, A. Riotto, F. Sala, A. Strumia and A. Urbano, *Weak corrections are relevant for dark matter indirect detection*, *JCAP* **03** (2011) 019 [1009.0224].
- [76] N. Fischer, S. Prestel, M. Ritzmann and P. Skands, *VINCIA for hadron colliders*, *Eur. Phys. J. C* **76** (2016) 589 [1605.06142].
- [77] M. Backović, K. Kong and M. McCaskey, *MadDM v.1.0: Computation of dark matter relic abundance using MadGraph 5*, *Phys. Dark Univ.* **5–6** (2014) 18–28.
- [78] S. Amoroso, S. Caron, A. Jueid, R. Ruiz de Austri and P. Skands, *Estimating QCD uncertainties in Monte Carlo event generators for gamma-ray dark matter searches*, *JCAP* **2019** (2019) 007 [1812.07424].
- [79] G. Breit and J.A. Wheeler, *Collision of Two Light Quanta*, *Phys. Rev.* **46** (1934) 1087.
- [80] O. Klein and T. Nishina, *Über die Streuung von Strahlung durch freie Elektronen nach der neuen relativistischen Quantendynamik von Dirac*, *Zeitschrift für Physik* **52** (1929) 853.
- [81] H. Cheng and T.T. Wu, *Cross sections for two-pair production at infinite energy*, *Phys. Rev. D* **2** (1970) 2103.
- [82] S.A. Bonometto and P. Marcolungo, *Metagalactic opacity to photons of energy larger than 10-to-the-17 ev*, *Lett. Nuovo Cim.* **5S2** (1972) 595.
- [83] C. Heiter, D. Kuempel, D. Walz and M. Erdmann, *Production and propagation of*

- ultra-high energy photons using CRPropa 3, *Astropart. Phys.* **102** (2018) 39 [1710.11406].
- [84] R. Alves Batista and A. Saveliev, *The Gamma-Ray Window to Intergalactic Magnetism*, *Universe* **7** (2021) 223 [2105.12020].
- [85] A. Saldana-Lopez, A. Domínguez, P.G. Pérez-González, J. Finke, M. Ajello, J.R. Primack et al., *An observational determination of the evolving extragalactic background light from the multiwavelength HST/CANDELS survey in the Fermi and CTA era*, *Mon. Not. Roy. Astron. Soc.* **507** (2021) 5144 [2012.03035].
- [86] I.C. Nițu, H.T.J. Bevens, J.D. Bray and A.M.M. Scaife, *An updated estimate of the cosmic radio background and implications for ultra-high-energy photon propagation*, *Astropart. Phys.* **126** (2021) 102532 [2004.13596].
- [87] W. Kang, H.S. Hwang, H. Song, C. Park, N. Hwang and B.-G. Park, *A Deep Redshift Survey of the Perseus Cluster (A426): Spatial Distribution and Kinematics of Galaxies*, *Astrophys. J. Suppl.* **272** (2024) 22 [2403.19307].
- [88] J.D. Finke, L.C. Reyes, M. Georganopoulos, K. Reynolds, M. Ajello, S.J. Fegan et al., *Constraints on the Intergalactic Magnetic Field with Gamma-Ray Observations of Blazars*, *Astrophys. J.* **814** (2015) 20 [1510.02485].
- [89] R.J. Protheroe and P.A. Johnson, *Propagation of ultrahigh-energy protons over cosmological distances and implications for topological defect models*, *Astropart. Phys.* **4** (1996) 253 [astro-ph/9506119].
- [90] S. Lee, *On the propagation of extragalactic high-energy cosmic and gamma-rays*, *Phys. Rev. D* **58** (1998) 043004 [astro-ph/9604098].
- [91] B. Namumba, C. Carignan, S. Passmoor and W.J.G. de Blok, *H I kinematics, mass distribution and star formation threshold in NGC 6822, using the SKA pathfinder KAT-7*, *Mon. Not. Roy. Astron. Soc.* **472** (2017) 3761 [1708.09447].
- [92] J. Expósito-Márquez, C.B. Brook, M. Huertas-Company, A. Di Cintio, A.V. Macciò, R.J.J. Grand et al., *A probabilistic deep learning model to distinguish cusps and cores in dwarf galaxies*, *Mon. Not. Roy. Astron. Soc.* **519** (2023) 4384 [2209.05965].
- [93] M.A. Sánchez-Conde, M. Cannoni, F. Zandanel, M.E. Gómez and F. Prada, *Dark matter searches with Cherenkov telescopes: nearby dwarf galaxies or local galaxy clusters?*, *JCAP* **2011** (2011) 011 [1104.3530].
- [94] M.S. Mirakhor, S.A. Walker and J. Runge, *A detailed study of the bridge of excess X-ray emission between the galaxy clusters Abell 2029 and Abell 2033*, *Mon. Not. Roy. Astron. Soc.* **509** (2021) 1109 [2110.06224].
- [95] K. Abe, S. Abe, F. Acero, A. Acharyya, R. Adam, A. Aguasca-Cabot et al., *Prospects for γ -ray observations of the Perseus galaxy cluster with the Cherenkov Telescope Array*, *JCAP* **10** (2024) 004 [2309.03712].
- [96] G. Di Marco, R. Alves Batista and M.A. Sánchez-Conde, *Revisiting the propagation of highly-energetic gamma rays in the Galaxy*, *Phys. Rev. D* **111** (2025) 083004 [2408.08818].